H-aggregates Granting Crystallization Induced Emissive Behavior and Ultralong Phosphorescence from a Pure Organic Molecule

Elena Lucenti,[a] Alessandra Forni,[a] Chiara Botta,[b] Lucia Carlucci,[c] Clelia Giannini,[c] Daniele Marinotto,[c] Andrea Previtali,[c] Stefania Righetto[c] and Elena Cariati[c,]*

a) ISTM-CNR, Istituto di Scienze e Tecnologie Molecolari – Consiglio Nazionale delle Ricerche and INSTM UdR, via Golgi 19, 20133 Milano, Italy.

b) ISMAC-CNR, Istituto per lo Studio delle Macromolecole - Consiglio Nazionale delle Ricerche and INSTM UdR, Via Corti 12, 20133 Milano, Italy.

c) Department of Chemistry, Università degli Studi di Milano and INSTM UdR, via Golgi 19, 20133 Milano, Italy.

AUTHOR INFORMATION

Corresponding Author

* Email: elena.cariati@unimi.it

ABSTRACT Solid state luminescent materials with long lifetimes are the subject of ever growing interest both from a scientific and a technological point of view. However, when dealing with organic compounds, the achievement of highly efficient materials is limited by aggregation caused quenching (ACQ) phenomena on one side and by ultrafast deactivation of the excited states on the other. Here, we report on a simple organic molecule, namely cyclic triimidazole ($C_9H_6N_6$), **1**, showing crystallization induced emissive (CIE) behavior and, in particular, ultralong phosphorescence due to strong coupling in H-aggregated molecules. Our experimental data reveal that luminescence lifetimes up to 1 s, which are several orders of magnitude longer than those of conventional organic fluorophores, can be realized under ambient conditions thus expanding the class of organic materials for phosphorescence applications.

TOC GRAPHICS

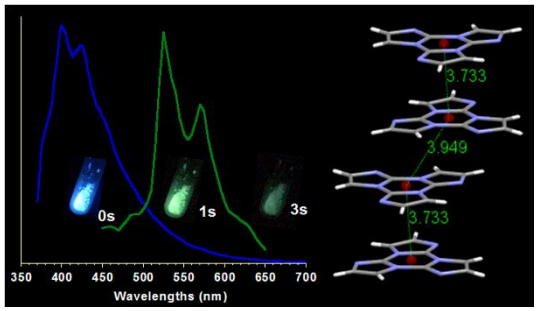

KEYWORDS Organic room temperature phosphorescence, Photophysics, Time-resolved spectroscopy, Ultralong phosphorescence

Solid-state luminogens have been the subject of great interest because high tech applications of light emitting materials very often require their use in the condensed phase. Unfortunately, frequently, weakly or even non-emissive solid materials are obtained from highly emissive molecules due to the notorious Aggregation Caused Quenching (ACQ) phenomenon. However, since the pioneering work of Tang,[1] many efforts have been spent on the isolation of compounds characterized by enhanced emission in the solid (crystalline and amorphous) state, referred to as Aggregation Induced Emission (AIE). In this regard, even more intriguing are some non-emissive molecules which are induced to emit by crystallization (Crystallization Induced Emission; CIE) but not amorphization. In these systems specific features of the crystal packing play a key role on the emissive properties of the crystal-phase materials.[2]

In parallel, a strong effort has been devoted to the search of organic molecules with long-lived excited states which enable exciton migration over long distances for increased production of free charges.[3-6] Usually, to enhance the transition from singlet (short-lived) to triplet (long-lived) states, either inorganic metals or special organic moieties (for example, aromatic aldehyde, heavy halogen and deuterated carbon) are required. In addition, since the triplet excitons generated in organic molecules are highly sensitive to oxygen and temperature, stringent conditions are required to observe long lived phosphorescence from pure organic molecules. However, very recently, An *et al.* reported ultra-long phosphorescent emission features in structures of planar organic molecules coupled in H-aggregates, which provide an effective means of stabilizing and protecting the triplet excitons formed through intersystem crossing.[7] The stabilized excited state, which functions as an energy trap at a lower energy level, may

delocalize on several neighboring molecules, offering suppressed radiative and non-radiative deactivation decay rates in favour of long-lived excited states and ultralong phosphorescence. This feature is particularly intriguing owing to the commonly accepted view of H-aggregates as non-emissive in character, in contrast with many J-aggregates, though some papers have appeared reporting about highly emissive fluorescent H-aggregates.[8-10]

Here we report a simple pure organic molecule which is weakly emissive in solution but highly so in crystals. The nature of the emission is verified by time resolved emission spectroscopy revealing the presence of both fluorescence and phosphorescence, this latter showing an impressive ultralong lifetime (up to 1 s at room temperature in air). By combined experimental, structural and theoretical calculations, the crystallization induced ultralong phosphorescence of the compound is attributed to its H-aggregation.

Cyclic triimidazole (triimidazo[1,2-*a*:1',2'-*c*:1",2"-*e*][1,3,5]triazine), **1**, was prepared, together with minor amounts of isomeric by-product (separated by column chromatography) **2** (triimidazo[1,2-*a*:1',2'-*c*:1",5"-*e*][1,3,5]triazine) (Scheme 1), as described in the literature.[11,12] Both **1** and **2** are poorly emissive in solution but their powders are brightly so under an UV lamp. Starting from this key observation we have performed a full photophysical characterization of the two.

Scheme 1. Structure of the two isomeric cyclic triimidazoles **1** and **2**.

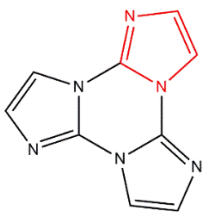

1

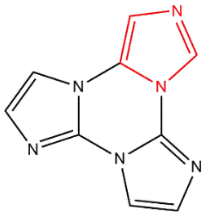

2

Diluted solutions of **1** (10^{-4}-10^{-5} M) in good solvents (DCM, toluene, etc) display an absorption (230 nm, Fig. S1) and a weak emission even under nitrogen (10^{-4} M in DCM, 390 nm, photoluminescence quantum efficiency (Φ) = 2% at r.t. in air).

The emission is slightly intensified only by forcing aggregation through addition of a non solvent (hexane or pentane) in a v/v 50:50 ratio (Fig. S2), while retaining a low concentration. However, very highly concentrated DCM solutions (10^{-2} M) show an additional very weak red shifted absorption band (345 nm) (Fig. S3) and a remarkable intensification of the emission (400 nm, τ best fitted as a triexponential = 0.15, 2.42 and 7.84 ns, Fig. S4, Table 1) corresponding to a band in the excitation spectrum at 325 nm (Fig. S5). These observations suggest that aggregation itself is not sufficient to switch on luminescence and that proper molecules' organization is a *conditio sine qua non* to observe emission from **1**.

Surprisingly, by cooling the 10^{-2} M DCM solution at 77K in air (Fig. 1) a broader emission band (λ_{max} = 435 nm) is observed due to the coexistence of a predominant prompt (τ triexponential = 0.99, 4.35 and 15.68 ns) and a longer wavelength (500 nm) delayed component with ultralong lifetimes (τ triexponential = 8, 115 and 939 ms measured at 570 nm, Table 1) (Fig. S6).

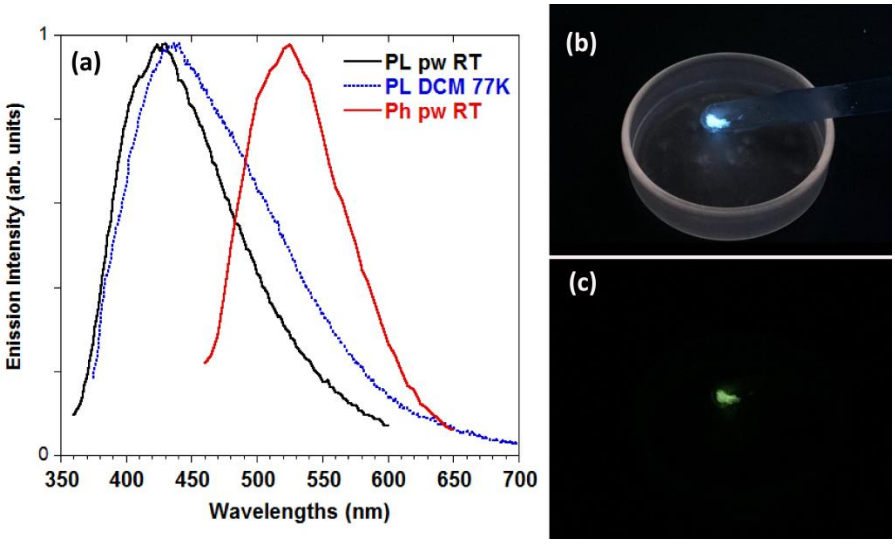

Figure 1. a) Photoluminescence of the DCM solution (10^{-2}M, λ_{exc}=350 nm) at 77K (blue dotted line). Photoluminescence (black line, λ_{exc}=330 nm) and phosphorescence (red line, time delay 172 ms, λ_{exc}=374 nm) of powders at 298 K. Pictures of powders at 77K with UV on (b) and off (c).

Based on these observations, we undertook the investigation of solid **1**. Powders of the compound display an intense blue emission under UV light but, surprisingly, upon removal of the UV source the emission color changes into green and slowly fades with a remarkably long luminescence lifetime, revealing, in general, crystallization emissive and, in particular, crystallization induced phosphorescence (CIP) behavior. To deeper investigate this CIE behavior we performed steady state and time resolved emission measurements both at r.t and 77 K.

When excited at 350 nm, microcrystalline powders of **1** (obtained from DCM solution by evaporation in vacuum at 10^{-2} Torr, see XRPD pattern in Fig. S21) display at room temperature a strong, broad, featureless emission centered at 425 nm (Φ = 18%, Fig. 1). Time resolved emission experiment indicated the presence of a prompt (τ biexponential = 3.49 and 10.89 ns)

and a longer wavelength (520 nm, Fig. 1) ultralong delayed component (τ triexponential = 12, 57 and 615 ms) which lasts for about 900 ms (Fig. S7 and S8). Emission experiment at 77 K revealed the presence of a prompt (430 nm, τ biexponential = 2.97ns, 13.24 ns) and a longer wavelength (525 nm) ultralong delayed component (τ triexponential = 10, 200 and 969 ms) which lasts for about 3.6 s (Fig. S9-S10, Table 1). In addition, almost identical steady-state photoluminescence spectra and lifetime measurements of the compound in solid state were obtained in different media (nitrogen and air), revealing an inertness of the triplet excited states to oxygen. However, we observed that both the shape of the emission and the absolute quantum yield are sensitive to the degree of crystallinity of the sample. In fact, crystals of **1** (obtained by slow evaporation from DCM solution) emit with Φ equal to 30%. Vibronic components appear both in the prompt (400, 424 nm) and in the time resolved delayed emission (525, 570 nm) which now lasts for 3.6 s (τ triexponential = 10, 52 and 990 ms) (Fig. 2, S11-S12, Table 1), a behavior very similar to that of the microcrystalline powder at 77K.

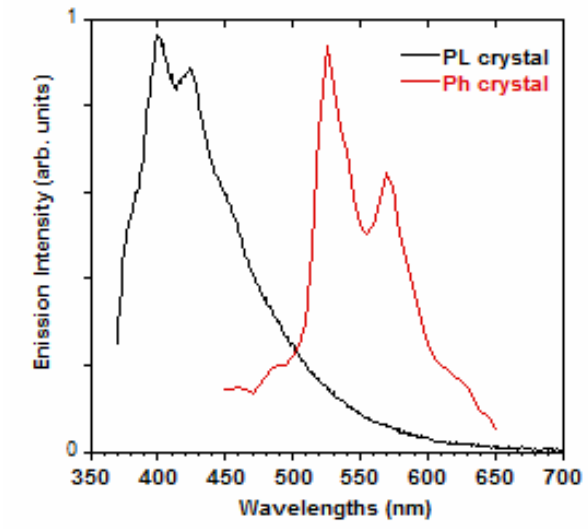

Figure 2. Photoluminescence (black line, λ_{exc}=350 nm) and phosphorescence (red line, time delay 472 ms, λ_{exc}=374 nm) of the crystals at 298 K.

Accordingly, a decrease in Φ (22 %) and the loss of the vibronic components is observed when crystals are ground in a mortar, revealing mechanochromic behavior.[13-15]

In addition, single crystals of **1** show polarized emission with polarization orthogonal to the long axis of the crystal (Fig. 3) when excited with unpolarized UV light, indicating that the transition dipole moment is oriented orthogonal to the long axis of the crystal. The crystal surfaces display bright emission due to wave-guiding effects.

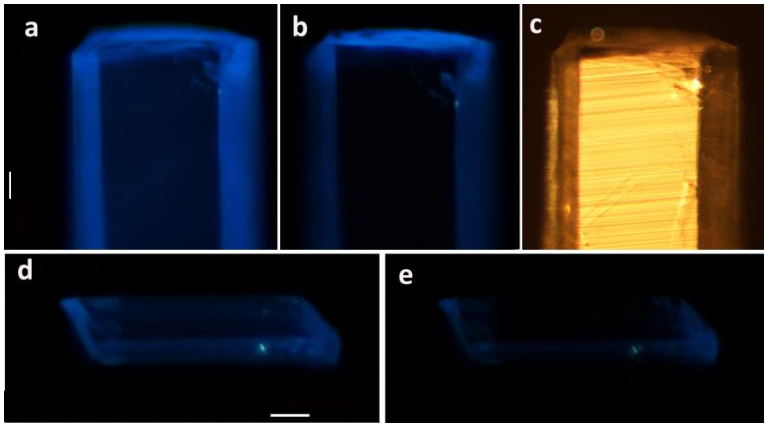

Figure 3. Microscopy images of a part of a crystal under unpolarized UV light taken with an analyzer with the transmission axis horizontal (a), vertical (b) and under white light (c). Images of a smaller crystal under unpolarized UV light taken with the analyzer with the transmission axis vertical (d) and horizontal (e). White bars are 30 micron long.

The X-ray crystal structure of **1**[11] evidences that molecules are slightly twisted with respect to an idealized D_{3h} symmetry. Very weak C–H···N hydrogen bonds connect the molecules along planar rows, laterally connected through other C–H···N hydrogen bonds to form approximated sheets. Along the third direction, molecules of **1** stack in face-to-face anti-parallel-packed zigzag columns with distances between average molecular planes alternately equal to 3.204(9) and 3.290(10) Å, and corresponding distances between centroids of the central rings equal to 3.95 and 3.73 Å, respectively (Fig. 4, left).

Such short distances are indicative of strong π-π interactions in the ground state, associated with large interchromophoric π-stacking area and formation of H-aggregates.

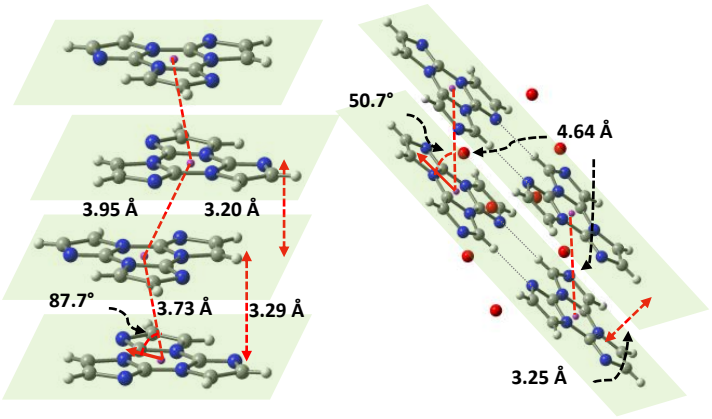

Figure 4. Fragment of crystal packing of **1** (left) and **2** (right) showing the key intermolecular distances and the angles between the transition moment dipoles (red arrows) and the axis through the centroids of the triazinic rings (purple circles).

Table 1. Room and low temperature emission maxima, photoluminescence quantum efficiency (Φ) and lifetimes of **1** and **2**.

Sample	298 K			77 K	
	Φ	**λ_{em} (nm)**	**τ (%)**	**λ_{em} (nm)**	**τ (%)**
1 (DCM)	2%[a]	400[b]	τ_1 0.15 ns (4.4)[c] τ_2 2.42 ns (32.3)[c] τ_3 7.84 ns (63.3)[c]	435[b]	τ_1 0.99ns (5.4)[e] τ_2 4.35 ns (30.3)[e] τ_3 15.68 ns (64.3)[e]
			τ_1 0.21 ns (10.9)[d] τ_2 1.45 ns (28.1)[d] τ_3 7.25 ns (61.0)[d]	500[b]	τ_1 8.32ms (2.6)[d] τ_2 114.8 ms (10.5)[d] τ_3 939 ms (86.9)[d]
1 (powder)[f]	18%	425	τ_1 3.49 ns (32.9)[c] τ_2 10.89ns (67.1)[c]	430	τ_1 2.97ns (30.6)[c] τ_2 13.24ns (69.4)[c]
		520	τ_1 11.49ms (29.0)[d] τ_2 57.29ms (37.2)[d] τ_3 614.56ms (33.8)[d]	520	$\tau_1$10ms (0.88)[g] τ_2 200ms (3.69)[g] τ_3 969.33ms (95.5)[g]
1 (crystals)	30%	400	τ_1 0.17ns (81.0)[h] τ_2 2.84ns (16.2)[h] τ_3 15.29ns (2.8)[h]	403	τ_1 1.71ns (69.6)[c] τ_2 9.49 ns (30.4)[c]
		525	τ_1 10ms (10.2)[d] τ_2 52ms (24.9)[d] τ_3 990ms (64.9)[d]	510	τ_1 510 ms (14.3)[g] τ_2 1118 ms (85.7)[g]
2 (crystals)	13%	415	τ_1 1.26ns (70.5)[c] τ_2 4.21ns (29.5)[c]	420	τ_1 4.48ns (60.6)[e] τ_2 18.17ns (39.4)[e]
			τ_1 3.9ns (64.6)[g] τ_2 13.88ns (35.4)[g]		τ_1 5.54 ns (73.0)[g] τ_2 22.28ns (27.0)[g]

[a]10^{-4}M; [b]10^{-2}M; [c]measured at 420 nm; [d]measured at 570 nm; [e]measured at 450 nm; [f]microcrystalline powders obtained by fast DCM evaporation; [g]measured at 540 nm; [h]measured at 400 nm.

To probe the mechanism underlying the observed emissive behavior of **1**, a DFT and TDDFT investigation on molecular scale has been performed. Geometry optimization of **1** provides a minimum having an almost perfect C_{3h} symmetry, while optimization of stacked aggregates (dimer and tetramer, see Fig. S13) led to stable minima where the monomers lack such symmetry. This confirms that intermolecular π-π stacking interactions are responsible for the observed molecular distortion (interaction energy for the dimer = 10.11 kcal/mol).

The simulated absorption spectrum of the optimized monomer consists of only two significant transitions, $S_0 \rightarrow S_3$ and $S_0 \rightarrow S_4$, both computed at 203 nm (207 nm in DCM) with oscillator strength f=0.56 and described as $\pi \rightarrow \pi^*$ transitions, with the involved frontier orbitals delocalized over the whole molecule (Fig. S14). They correspond to the strong absorption band observed in DCM solution at 230 nm (Fig. S1). The $S_0 \rightarrow S_1$ transition, on the other hand, is computed at 228 nm with virtually zero oscillator strength and $\pi \rightarrow \pi^*$ character. Similar features are obtained for the π-π stacked dimer and tetramer of **1** (two strong transitions at 200-203 nm and, respectively, two and four almost degenerate weak transitions at 228-230 nm), but the oscillator strengths of the weaker transitions slightly increase with increasing the dimensionality of the aggregate (f=0.0007 and 0.0011 for the dimer and the tetramer, respectively). Such trend is in agreement with the weak absorption/excitation band observed in highly concentrated DCM solutions. Its weakness could be explained by the chromophore's high symmetry and may be then interpreted as a symmetry-forbidden transition. Such a high symmetry is approximately preserved in dilute solutions (as indicated by monomer calculations), but partially disrupted when intermolecular forces arising from the aggregate state come into play, allowing intensification of the $S_0 \rightarrow S_1$ transition. The associated transition dipole moment is found to lie in the molecular plane.

Referring to the X-ray structure, it forms an angle of 87.7° with the axis through the centroids of the triazinic ring (Fig. 4), confirming the H-type nature of the crystalline aggregates of **1**.[16]

Aggregation is predicted to be as well responsible of the observed enhancement of the fluorescence when going from solution to the solid state. Optimization of the S_1 excited state of the monomer and dimer of **1**, in fact, leads to stationary states at 249 and 276 nm, respectively, characterized by significantly increased (from 0 to 0.086) oscillator strengths going from the monomer to the dimer. The nature of the excited emissive states of **1** has been investigated by determining the set of the first excited triplet states for the monomer and the dimer to compare their energy with that of S_1,[7,17,18] since it is known that intersystem crossing (ISC) is promoted by low energy gaps between the two states involved. For the monomer, up to six triplet states (T_1-T_6) lye below S_1, three of them having similar transition configurations to that of S_1 and lying within 0.35 eV from it (Fig. 5, left).

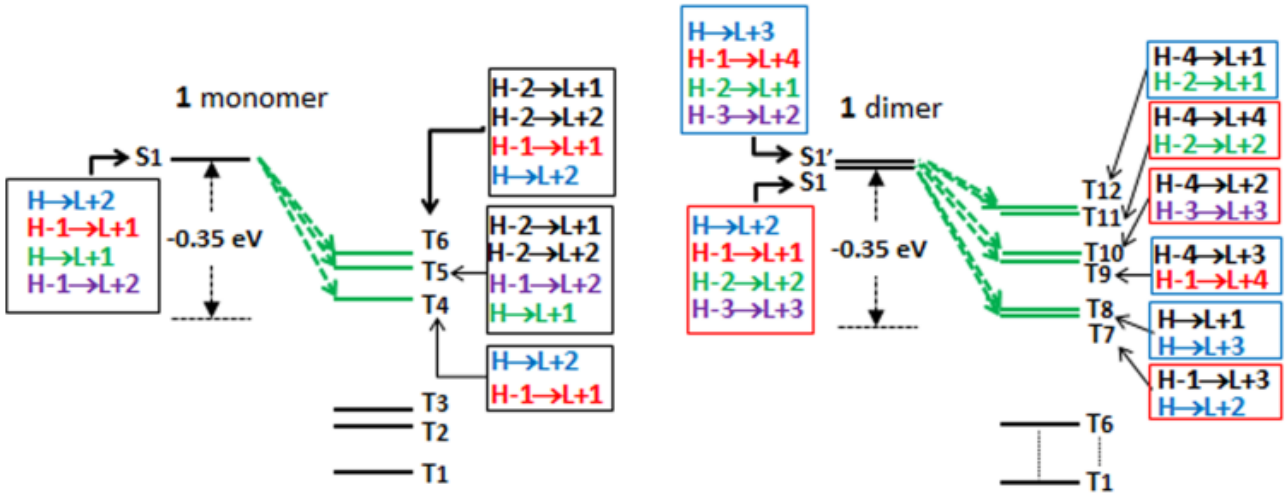

Figure 5. Schematic diagram of singlet and triplet TD-ωB97X/6-311++G(d,p) energy levels and main orbital configurations of a monomer (left) and dimer (right) of **1**. The green dashed arrows correspond to the ISC processes probably occurring from the S_1 state to the closest lower-lying triplet states (T_n).

Calculations on the dimer provide an increased number of triplet states below S_1 (and the degenerate S_1' state), T_1-T_{12}, as obviously expected owing to the strong intermolecular interaction, six of them having transition configurations similar to S_1 and S_1', and close to them within 0.35 eV (Fig. 5, right), implying a smaller S-T energy gap. This indicates enhanced ISC for the dimer with respect to the monomer, supporting the higher ISC probability to populate triplet excited in the H-aggregate phase. As previously demonstrated,[7] this type of aggregation together with the (π,π*) character of the triplet emitting state, which increases its lifetime owing to the poor spin-orbit coupling with the singlet states,[3] might provide an effective stabilization of the triplet excitons necessary for ultralong phosphorescence.

To confirm this hypothesis on the key role of H aggregates in **1**, we have isolated and characterized (including single crystal X-ray structure determination,[19] Fig. S19) its isomer, **2**. This compound crystallizes as hydrated phase with CIE behavior, being very poorly emissive in solution (10^{-4} M in DCM Φ 2.8% at r.t. in air) but quite so in crystals (λ_{max} = 415 nm, Φ = 13%) (Fig. S15), with emission characterized by fast de-excitation (in the ns region, see S16 and Table 1), which is red-shifted to 420 nm at 77 K (Fig. S17). However, no longer lifetime emissive component is observed for such emission even at low temperature (77 K, Fig. S18, Table 1). By looking at its crystal structure, a distortion from planarity quite similar to that of **1** is observed. Crystal packing, on the other hand, is completely different, revealing herringbone aggregation of π-π stacked ribbons formed by dimeric units interconnected through cyclic C–H···N hydrogen bonds and joined each other by the cocrystallized water molecules (Fig. 4, right). The dimeric units form face-to-face parallel-packed slipped column with distances between average molecular planes equal to 3.250 Å, and distance between centroids of the central rings equal to

4.65 Å. The greater slippage compared to that of **1** suggests the presence of weaker π-π interactions. Moreover, the transition dipole moment forms an angle of 50.7° with the axis through the centroids of the triazinic ring (Fig. 4). Such loss of H-aggregation in this structure is in line with its lacking of the ultralong emission component. The role of aggregation in tuning the different emissive properties of **1** and **2** in crystal phase is further supported by theory. Calculations on **2** provide molecular properties[20] rather similar to those of **1**, as observed experimentally. However, differently from **1,** simulations fail to model the aggregate form of **2**, since a much shorter intermolecular distance for the optimized dimer with respect to the experimental value (see SI) was found owing to the lack, in calculations, of the cocrystallized water molecules.

In conclusion, we have prepared and fully characterized a very simple organic molecule, cyclic triimidazole ($C_9H_6N_6$), **1**, able to display crystallization induced and mechanochromic emissive behaviour, together with visible ultralong luminescence (1 s) at ambient conditions associated with H-aggregation. This compound open up to a new family of next-generation organic phosphors.

ASSOCIATED CONTENT

Supporting Information. Experimental details, absorption, emission and excitation spectra, fluorescence decays and additional theoretical results; CIF and checkcif of compound **2**.

ACKNOWLEDGMENT

The use of instrumentation purchased through the Regione Lombardia – Fondazione Cariplo joint SmartMatLab Project is gratefully acknowledged. C.B. would like to thank ACCORDO QUADRO Regione Lombardia project (decreto 7784/2016) gI-ZEBh for partial financial support.

REFERENCES

(1) Luo, J. D.; Xie, Z. L.; Lam, J. W. Y.; Cheng, L.; Chen, H. Y.; Qiu, C. F.; Kwok, H. S.; Zhan, X. W.; Liu, Y. Q.; Zhu, D. B.; et al. Aggregation-induced emission of 1-methyl-1,2,3,4,5-pentaphenylsilole. *Chem. Commun.* **2001**, 1740-1741.

(2) Cariati, E.; Lanzeni, V.; Tordin, E.; Ugo, R.; Botta, C.; Giacometti Schieroni, A.; Sironi, A.; Pasini, D. Efficient crystallization induced emissive materials based on a simple push–pull molecular structure. *Phys. Chem. Chem. Phys.* **2011**, *13*, 18005–18014.

(3) Baroncini, M.; Bergamini, G.; Ceroni, P. Rigidification or interaction-induced phosphorescence of organic molecules. *Chem. Commun.* **2017**, *53*, 2081-2093.

(4) Zhao, W.; He, Z.; Lam, J.W.Y.; Peng, Q.; Ma, H.; Shuai, Z.; Bai, G.; Hao, J.; Tang, B. Z. Rational Molecular Design for Achieving Persistent and Efficient Pure Organic Room-Temperature Phosphorescence. *Chem* **2016**, *1*, 592–602.

(5) Wei, J.; Liang, B.; Duan, R.; Cheng, Z.; Li, C.; Zhou, T.; Yi, Y.; Wang, Y. Induction of Strong Long-Lived Room-Temperature Phosphorescence of N-Phenyl-2-naphthylamine

Molecules by Confinement in a Crystalline Dibromobiphenyl Matrix. *Angew. Chem. Int. Ed.* **2016**, *55*, 1–7.

(6) Yuan, W. Z.; Shen, X. Y.; Zhao, H.; Lam, J. W. Y.; Tang, L.; Lu, P.; Wang, C.; Liu, Y.; Wang, Z.; Zheng, Q.; et al. Crystallization-Induced Phosphorescence of Pure Organic Luminogens at Room Temperature. *J. Phys. Chem. C* **2010**, *114*, 6090–6099.

(7) An, Z.; Zheng, C.; Tao, Y.; Chen, R.; Shi, H.; Chen, T.; Wang, Z.; Li, H.; Deng, R.; Liu, X.; et al. Stabilizing triplet excited states for ultralong organic phosphorescence. *Nat. Mater.* **2015**, *14*, 685-690.

(8) Rösch, U.; Yao, S.; Wortmann, R.; Würthner, F. Fluorescent H-Aggregates of Merocyanine Dyes. *Angew. Chem. Int. Ed.* **2006**, *45*, 7026–7030.

(9) Basak, S.; Nandi, N.; Bhattacharyya, K.; Datta, A.; Banerjee, A. Fluorescence from an H-aggregated naphthalenediimide based peptide: photophysical and computational investigation of this rare phenomenon. *Phys. Chem. Chem. Phys.* **2015**, *17*, 30398-30403.

(10) Bayda, M.; Dumoulin, F.; Hug, G. L.; Koput, J.; Gorniak, R.; Wojcik, A. Fluorescent H-aggregates of an asymmetrically substituted mono-amino Zn(II) phthalocyanine. *Dalton Trans.* **2017**, *46*, 1914-1926.

(11) Schubert, D. M.; Natan, D. T.; Wilson, D. C.; Hardcastle, K. I. Facile Synthesis and Structures of Cyclic Triimidazole and Its Boric Acid Adduct. *Cryst. Growth Des.* **2011**, *11*, 843-850.

(12) Buck, D. M.; Kunz, D. Triazine Annelated NHC Featuring Unprecedented Coordination Versatility. *Organometallics* **2015**, *34*, 5335-5340.

(13) Li, C.; Tang, X.; Zhang, L.; Li, C.; Liu, Z.; Bo, Z.; Dong, Y. Q.; Tian, Y. H.; Dong, Y.; Tang, B. Z. Reversible Luminescence Switching of an Organic Solid: Controllable On–Off Persistent Room Temperature Phosphorescence and Stimulated Multiple Fluorescence Conversion. *Adv. Optical Mater.* **2015**, *3*, 1184–1190.

(14) Gong, Y.; Chen, G.; Peng, Q.; Yuan, W. Z.; Xie, Y.; Li, S.; Zhang, Y.; Tang, B. Z. Achieving Persistent Room Temperature Phosphorescence and Remarkable Mechanochromism from Pure Organic Luminogens. *Adv. Mater.* **2015**, *27*, 6195–6201.

(15) Botta, C.; Benedini, S.; Carlucci, L.; Forni, A.; Marinotto, D.; Nitti, A.; Pasini, D.; Righetto, S.; Cariati, E. Polymorphism-dependent aggregation induced emission of a push–pull dye and its multi-stimuli responsive behavior. *J. Mater. Chem. C* **2016**, *4*, 2979-2989.

(16) Kasha, M.; Rawls, H. R.; El-Bayoumi, M. A. The exciton model in molecular spectroscopy. *Pure Appl. Chem.* **1965**, *11*, 371-392.

(17) Englman, R.; Jortner, J. The energy gap law for radiationless transitions in large molecules. *Mol. Phys*. **1970**, *18*, 145-164.

(18) Yang, L.; Wang, X.; Zhang, G.; Chen, X.; Zhang, G.; Jiang, J. Aggregation-induced intersystem crossing: a novel strategy for efficient molecular phosphorescence. *Nanoscale* **2016**, *8*, 17422–17426.

(19) Crystals of **2** suitable for X-ray data collection were obtained by slow evaporation at room temperature in air of a 0.06 M solution of **2** in CH_3CN. Crystal data: $C_9H_6N_6 \cdot H_2O$

(MW=216.21), monoclinic $P2_1/c$, a=4.6470(7), b=18.557(3), c=11.5180(17) Å, β=91.618(2)°, V=992.9(3) $Å^3$.

(20) TDDFT calculations provide a weak $S_0 \rightarrow S_1$ transition at 229 nm with $\pi \rightarrow \pi^*$ character and oscillator strength (*f*=0.032) slightly greater than that of **1**, in agreement with its symmetry loss, and strong $S_0 \rightarrow S_2$, $S_0 \rightarrow S_3$ and $S_0 \rightarrow S_4$ transitions at 216 (*f*=0.27), 202 (*f*=0.34) and 199 (*f*=0.35) nm.